

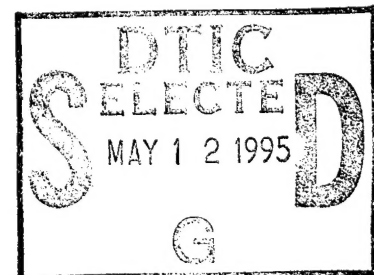
# NATIONAL AIR INTELLIGENCE CENTER



HIGH POWER CO<sub>2</sub> LASER WINDOWS AND REFLECTION REDUCING COATINGS

by

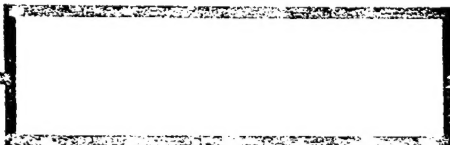
G.A. Atanassov, Gu Peifu, et al.



DTIC QUALITY INSPECTED 5

19950512 060

Approved for public release;  
Distribution unlimited.



NAIC- ID(RS)T-0760-94

**HUMAN TRANSLATION**

NAIC-ID(RS)T-0760-94

10 April 1995

MICROFICHE NR: 95C000174

HIGH POWER CO<sub>2</sub> LASER WINDOWS AND REFLECTION REDUCING COATINGS

By: G.A. Atanassov, Gu Peifu, et al.

English pages: 13

Source: Guangxue Xuebao, Vol. 12, Nr. 10, October 1992;  
pp. 934-940

Country of origin: China

Translated by: SCITRAN

F33657-84-D-0165

Requester: NAIC/TATD/Bruce Armstrong

Approved for public release; Distribution unlimited.

Accession For	
NTIS CRA&I	<input checked="" type="checkbox"/>
DTIC TAB	<input type="checkbox"/>
Unannounced	<input type="checkbox"/>
Justification	
By	
Distribution /	
Availability Codes	
Dist	Avail. and / or Special
A-1	

THIS TRANSLATION IS A RENDITION OF THE ORIGINAL FOREIGN TEXT WITHOUT ANY ANALYTICAL OR EDITORIAL COMMENT STATEMENTS OR THEORIES ADVOCATED OR IMPLIED ARE THOSE OF THE SOURCE AND DO NOT NECESSARILY REFLECT THE POSITION OR OPINION OF THE NATIONAL AIR INTELLIGENCE CENTER.

PREPARED BY:

TRANSLATION SERVICES  
NATIONAL AIR INTELLIGENCE CENTER  
WPAFB, OHIO

NAIC- ID(RS)T-0760-94

Date

10 April 1995

# GRAPHICS DISCLAIMER

All figures, graphics, tables, equations, etc. merged into this translation were extracted from the best quality copy available.

HIGH POWER CO<sub>2</sub> LASER WINDOWS AND REFLECTION REDUCING COATINGS

G.A. Atanassov Gu Peifu Liu Xu Tang Jinfa

Translation of "Da Gong Lyu CO<sub>2</sub> Ji Guang Qi Chaung Kou Ji Jian  
Fan She Mo"; ACTA OPTICA SINICA, Vol.12 No.10 Oct92, pp 934-940

Translated by

S C I T R A N

1482 East Valley Road

Santa Barbara, CA 93108

HIGH POWER CO<sub>2</sub> LASER WINDOWS AND REFLECTION REDUCING COATINGS<sup>1</sup>G.A. Atanasov<sup>2</sup> Gu Peifu Liu Xu Tang Jinfa

## ABSTRACT

This article describes evaluation standards for window materials. In conjunction with that, comparisons were made between the four types of materials Ge, GaAs, ZnSe, and KCl. It was discovered that KCl possesses optimum optical characteristics. In conjunction with this, reflection reducing films associated with good performance were designed and prepared. Measurements were done of their absorption and laser damage threshold values.

KEY WORDS Antireflection coating, Laser damage threshold

## 1 INTRODUCTION

Window materials used in infrared CO<sub>2</sub> lasers include semiconductor materials (for example, Ge, CdTe, GaAs, and ZnSe), dielectric materials (for example, KCl and NaCl), and infrared glass (for example, KRS-5). As far as research on these materials is concerned, there is already at least a 20 year history [1-4]. In 1986, Miyata pointed out that, due to KCl, at 1.06  $\mu\text{m}$ , they possess unusually low absorption coefficients ( $7 \times 10^{-5} \text{cm}^{-1}$ ) and unusually low absorption temperature coefficients ( $3.7 \times 10^{-6} / \text{cm}^\circ\text{C}$ ) [6]. KCl optical components are capable of being successfully used as windows in 5-20kW high power CO<sub>2</sub> lasers. However, ZnSe and GaAs--due to their thermal lens effects--are only capable of use in laser systems under 5kW power.

---

\* Numbers in margins indicate foreign pagination.  
Commas in numbers indicate decimals.

<sup>1</sup> Aided by the National Education Committee Outstanding Young Teachers Fund

<sup>2</sup> Visiting Bulgarian Scholar

This article stresses discussion of and research on four types of window material: Ge, GaAs, ZnSe, and KCl. Full comparative analysis was done on their characteristics in order to facilitate finding a type capable of being appropriate as a material for 20kW CW CO<sub>2</sub> laser systems. In the results, it was discovered that monocrystalline KCl is optimum window material for high power CO<sub>2</sub> laser systems. The only problem is the need to provide a reflection reducing film with good antimoisture properties and mechanical performance. Going a step further, a three layer reflection reducing film to use on KCl was designed and prepared. Using CO<sub>2</sub> laser photothermal deflection techniques, their absorption was measured. A relatively high damage threshold was obtained.

## 2 THEORETICAL BASIS

When high power laser beams go through window material, due to window material absorbing laser energy, its temperature rises, causing thermal expansion, heat stress, and changes in refraction indices, etc--that is, producing photothermal deformations. Speaking in terms of actual applications, it is necessary to effectively limit these changes (much less rupture), in order to prevent optical characteristics turning bad.

### 2.1 Rupture Caused by Mechanical Properties

Stresses endured by window materials include the two parts of thermal stress given rise to by mechanical stress and from temperature gradients. When the two sides of windows are subjected to different pressures, mechanical stresses will then be produced. Assuming window static pressure to be  $P$ , then, in order to prevent window rupture, the needed thickness  $l$  is [3]

$$l=0.86\tau(P\cdot S_f/\sigma_c)^{1/2}, \quad (1)$$

In the equation,  $\sigma_c$  is the minimum stress which causes windows not to be able to change back.  $S_f$  is the safety factor for preventing window rupture.  $r$  is the window radius. With regard to a window used in a vacuum chamber, static pressure differences are usually very large. This static pressure difference will cause windows to deform. The result will be that the focal length of the window  $F_w$  will give rise to changes. One has [3]

$$\left. \begin{aligned} F_w &= -\tau^2/(n-n_0)l \cdot B^2, \\ B &= (3/4)[P(1-\nu^2)/E](\tau/l)^3, \end{aligned} \right\} \quad (2)$$

In the equations,  $n$  and  $n_0$  are, respectively, window material and peripheral media indices of refraction.  $r$  and  $l$  are window radius and thickness.  $E$  and  $\nu$  are Young moduli and Poisson coefficients. Considered from the angle of optical deformation, in order to guarantee window effectiveness, the critical thickness  $l_c$  is [3]

$$l_c = 1.68\tau[(n-1)(P/E)^2(2\tau/\lambda)]^{1/5}. \quad (3)$$

Making equations equal (1) and (3) to each other--even if optical deformation and rupture effects possess the same importance--solving for  $\sigma_c$  gives material strength  $\sigma_{c0}$ .

$$\sigma_{c0} = 0.26PS, [(n-1)^{-1}(E/P)^2(\lambda/2\tau)]^{2/5}. \quad (4)$$

With regard to materials having relatively bad strengths, the minimum thicknesses for windows with  $\sigma_c < \sigma_{c0}$  are determined by antirupture factors. However, in the case of materials with relatively high strengths,  $\sigma_c < \sigma_{c0}$  optical deformations will become important factors.

Obviously, setting out in considerations from antirupture

angles, it is, then, required for window material thermal expansion to be small, optical absorption to be low, and rupture moduli to be large. Deutsch [7] brings up a quality factor "FOM" used in order to describe the rupture characteristics given rise to by heat in an edge cooled optical component. For windows with only body absorption, it is

$$FOM_{TF}^B = \sigma K / \alpha \cdot \beta_v \cdot E, \quad (5)$$

For windows with only surface absorption, it is

$$FOM_{TF}^S = \sigma K \tau / \alpha A_s E, \quad (6)$$

In the equations,  $\sigma$  is rupture modulus.  $K$  is thermal conductivity.  $\alpha$  is thermal expansion coefficient.  $\beta_v$  is body absorption coefficient.  $A_s$  is surface absorption rate. Due to the fact that actual windows always simultaneously show the existence of body absorption and surface absorption, as a result, an effective absorption rate  $A_e$  [7] is introduced, substituting in equation (6) for  $A_s$  to be

$$A_e = (1-R)A_{c1} + (1-R)\beta_v l + A_{c2} + 2A'_s, \quad (7)$$

In the equation,  $R$  is the rate of window reflection.  $A_{c1}$  and  $A_{c2}$  are, respectively, absorption rates for antireflection coatings on two boundary surfaces.  $A'_s$  is the absorption rate for window-coating layer boundaries. For an ideal reflection reducing film,  $R=0$ .  $A'_s$  is different, following along with different window materials. In the calculations in this article,

$$2A'_s = 1 \times 10^{-4}.$$

Stresses given rise to by temperature gradients  $\sigma_{cr}$  and critical values for differences between window center and edge temperatures have the relationship [3]

$$\Delta T_e = 2\sigma_{cr} / \alpha E. \quad (8)$$



## 2.2 Optical Characteristic Distortions Lead to by Thermal Properties

When laser beams uniformly illuminate edge cooled windows, or, when window center incident energies are far larger than the edges, window center thickness increases, producing positive focal lengths (convergence effects). With regard to ionic type crystals, window center refraction indices will be smaller than the edges, that is,  $-dn/dT$ . As a result, one obtains negative focal lengths (divergence effects). In the case of covalent bond crystals, this is just the reverse. Because of this, net focal length can be positive or negative. It can even be infinitely large. However, covalent bond crystals are always positive. The explanation for this is that ionic type crystal net optical distortions will generally be smaller than covalent bond crystals.

Sparus [1] and Deutsch [7] give a thermal distortion coefficient  $\chi$  used in order to describe optical distortions

$$\chi = (dn/dT) + (1-\nu)\alpha(n-1) + (n^3/6)\alpha P, \quad (9)$$

In the equation,  $P$ , is a photoelasticity coefficient. In equation (9), the first, second, and third quantities correspond, respectively, to the influences of temperature on refraction indices, thermal expansion, and stresses.

In the case of the materials studied by this article, the second quantity is always positive. The magnitude of 9 directly reflects the magnitude of optical distortion. For a laser beam with energy in a Gaussian distribution, window temperature distributions follow relationships between radii and time and are capable of going through solutions of nonstable state equations to obtain [8]

$$c\rho \frac{\partial}{\partial t} [\Delta T(\tau, t)] = \dot{q}(\tau) + K \nabla^2 [\Delta T(\tau, t)], \quad (10)$$

In the equation,  $c$  is specific heat.  $\rho$  is window material density.  $\dot{q}(\tau)$  is the energy flow entering unit volumes within unit time periods at locations a distance  $\tau$  from the center of windows.

Changes in laser light strength passing through windows can be written as

$$\Delta I(\tau) = I_0(\tau) - I(\tau) \approx I_0(\tau) \beta_v l.$$

In the equation,  $I_0(\tau)$  and  $I(\tau)$  are, respectively, energies incident and radiated out at locations  $\tau$  on windows. Due to  $\beta_v$  being very small, the result is that one has

$$\dot{q}(\tau) = [\Delta I(\tau)/l] = I_0(\tau) \beta_v, \quad (11)$$

With regard to Gaussian distribution laser beams are concerned, input strengths are

$$I_0(\tau) = (0.48 P_w / \pi \rho_0^2) \exp(-2\tau^2 / \rho_0^2), \quad (12)$$

In the equation,  $P_w$  is laser beam power.  $\rho_0$  is the Gauss radius, that is, the facula radius specified by  $e^{-2}$ . Taking equation (12) and substituting into (11), it is then possible to a solution for equation (10) which is [9]

$$\Delta T(\tau, t) = \frac{0.48 P_w A_s}{\pi \rho_0^2 c} \int_0^t \frac{1}{[1 + (2t'/t_0)]} \exp\left(\frac{-2\tau^2/\rho_0^2}{[1 + (2t'/t_0)]}\right) dt', \quad (13)$$

In the equation,  $t_0$  is a time constant for the setting up of thermal lenses. With  $t_0 = (\rho_0^2 \rho / 4K)$  the integrals described above can be written as a series form

$$\Delta T(\tau, t) = \frac{0.24 P_w A_s}{4\pi k l} \left\{ \ln \left( 1 + \frac{2t}{t_0} \right) + \sum_{m=1}^{\infty} \frac{(-2\tau^2/\rho_0^2)^m}{m m!} \left[ 1 - \left( \frac{1}{1 + (2t/t_0)} \right)^m \right] \right\}, \quad (14)$$

In the equation,  $m > 10$  terms can often be ignored. In the case of continuous laser beams, after time  $t > 120t_0$ , temperature distributions reach equilibrium. Because of this, use is made of equation (14). Substituting in  $t/t_0 = 120$ , it is possible to calculate the temperature difference  $\Delta T$  between window centers and edges. What is regrettable is that equation (14) is only accurate for  $(\tau/\rho_0) = 0 \sim 1$ . Otherwise, calculation results will have big errors.

On windows, temperature differences between centers and edges  $\Delta\phi$  given rise to by nonuniform heating can be written as [2]

$$\Delta\phi = (2\pi/\lambda) l \cdot \chi \cdot \Delta T \quad \text{or} \quad (\Delta\phi/2\pi) = (l/\lambda) \chi \cdot \Delta T, \quad (15)$$

As far as edge cooled windows are concerned, Deufsch [7] brought up optical distortion quality factors. For body absorption and surface absorption states they are, respectively

$$FOM_D^b = (\lambda \cdot K / \beta_0 \chi \tau), \quad (16)$$

$$FOM_D^s = (\lambda \cdot K / A_s \chi). \quad (17)$$

In the same way, it is possible to use equation (7)  $A_e$  to substitute for  $A_s$  to calculate  $FOM_D$ .

### 3 CHARACTERISTICS COMPARISONS

On the basis of the discussion above, it is then possible to make full analyses, calculations, and comparisons for the characteristics of Ge, GaAs, ZnSe, and KCl. Table 1 sets out the physical properties of four types of window material. Calculated thermal distortion coefficients  $\chi$  are set out in Table 2.

From Table 2, one can know that, among these four types of materials, only KCl possesses negative thermal distortion coefficients. Moreover, numerical values are very low. The result is that thermally caused optical distortions can be expected to clearly diminish. When laser light passes through these materials, KCl windows operate using negative lens forms. However, the other three types of materials are all positive lenses. Among the three types of materials associated with positive thermal distortion coefficients, ZnSe possesses relatively low refraction indices, temperature coefficients, thermal expansion, and thermal stress. The result is that  $\chi$  is relatively low. As far as GaAs is concerned, although it has negative thermal stresses, the values, however, are far from being able to compensate  $(dn/dT)$ . Moreover, Ge is the worst type.

Window thicknesses and radii are estimated from equation (1) and equation (3). Table 3 gives the calculation results for various types of parameters. With regard to the three types of materials Ge, GaAs, and ZnSe,  $\sigma_{\infty} \approx \sigma_0$  and optical distortions are clearly key contradictions. Thicknesses actually required should be larger than  $l_c$ . If one adopts  $s_f=4$ , then, actual thicknesses are approximately 1.5cm. In the case of KCl,  $\sigma_{c0} \gg \sigma_0$ , and mechanical rupture are key problems. Considering that it is used as laser cavity windows, pressures within cavities are smaller than 1Pa. This represents windows undergoing static pressure  $P > 15$  PSI. Because of this, the thickness is taken as 2.5cm. Window radii are considered starting from actual requirements. Due to 20kW CW  $CO_2$  laser beam radii being 3.5 - 4.5cm, radii are, for this reason, taken as 6cm.

TABLE 1. THE PHYSICAL PROPERTIES OF Ge, GaAs, ZnSe AND KCl

Parameter	Symbol	Units	Ge	GaAs <sup>[10]</sup>	ZnSe <sup>[10]</sup>	KCl
Refractive index at 10.6 $\mu\text{m}$	$n$	—	4.00	3.275	2.403	1.457
Temperature dependence of $n$	$\frac{dn}{dT}$	$/^{\circ}\text{C}$	277 <sup>[7]</sup>	149	64	-31.3 <sup>[11]</sup>
Thermal conductivity	$K$	$\text{W/cm}\cdot^{\circ}\text{C}$	0.59 <sup>[7]</sup>	0.48	0.18	0.0654 <sup>[7]</sup>
Expansion coefficient	$\alpha$	$10^{-6}/^{\circ}\text{C}$	6.1 <sup>[11]</sup>	5.7	7.6	36 <sup>[11]</sup>
Young's modulus	$E$	$10^6 \text{ PSI}$	14.9 <sup>[4]</sup>	12	9.7	4.3 <sup>[4]</sup>
Rupture modulus	$\sigma$	PSI	13500 <sup>[4]</sup>	20000	8000	640 <sup>[7]</sup>
Critical stress	$\sigma_c$	PSI	13500 <sup>[4]</sup>	20000 <sup>[4]</sup>	6100 <sup>[4]</sup>	330 <sup>[4]</sup>
Hardness	—	Knoop	850	750	130	7.2
Poisson's ratio	$\nu$	—	0.34 <sup>[7]</sup>	0.31	0.28	0.36 <sup>[7]</sup>
Elasto-Optic coefficient	$P_1$	—	0.27 <sup>[7]</sup>	-0.143	0.105	0.21 <sup>[12]</sup>
Specific heat	$c$	$\text{J/g}\cdot^{\circ}\text{C}$	0.310 <sup>[11]</sup>	0.325	0.356	0.680 <sup>[11]</sup>

TABLE 2. THE RESULTS FROM THE CALCULATION OF THE THERMAL DISTORTION COEFFICIENT

Parameter	Units	Ge	GaAs	ZnSe	KCl
$dn/dT$	$10^{-6}/^{\circ}\text{C}$	24.52	16.99	13.65	22.37
Thermal expansion ( $1+\nu$ ) $\alpha$ ( $n-1$ )	$10^{-6}/^{\circ}\text{C}$	17.57	-4.94	1.85	3.90
State of stress $n^2\alpha P_1/6$	$10^{-6}/^{\circ}\text{C}$	277.	149.	64.	-31.3
Thermal distortion coefficient acc. to (9) $\chi$	$10^{-6}/^{\circ}\text{C}$	319.09	161.05	79.50	-5.03

For Ge and GaAs, besides high absorption, window center and edge phase differences  $\Delta\phi$  are also unacceptable. Even if it is ZnSe, with regard to a laser beam of 20kW power, they are unattractively too high. Only KCl values are very low, and it possesses very high optical distortion quality factors. Therefore, without a doubt, considered from optical distortion, KCl is a type of unusually satisfactory material. However, KCl's antithermal rupture quality factor is too small. Critical temperatures are also too low. These deficiencies require the use of a cooling system for added improvement. KCl crystals also have a deficiency which is bad moisture resistance. Because of this, a reflection reducing film which provides good protective properties is needed.

/938

TABLE 3. THE CALCULATED DESIGN PARAMETERS

Design parameter	Symbol	Units	Ge	GaAs	ZnSe	KCl
Required thickness acc. to (1)	$l$	cm	0.35	0.29	0.52	2.22
Critical thickness acc. to (3)	$l_c$	cm	0.33	0.34	0.33	0.37
Strength of equal importance	$\sigma_{\infty}$	$10^8$ PSI	15.3	14.4	14.7	12.0
Chosen thickness	$l$	cm	1.5	1.5	1.5	2.5
Chosen radius	$r$	cm	6	6	6	6
Volume absorption coefficient	$\beta_v$	$\text{cm}^{-1}$	$2 \times 10^{-2(11)}$	$7.4 \times 10^{-3(10)}$	$5.7 \times 10^{-4(10)}$	$1.8 \times 10^{-4}$
Absorptance for AR Coatings	$(1-R)A_{c1}+A_{c2}$	—	$8 \times 10^{-4}$	$8 \times 10^{-4}$	$1.1 \times 10^{-3}$	$3 \times 10^{-4}$
Effective absorptance	$A_e$	—	0.031	0.012	0.002	0.0009
Temperature difference	$\Delta T$	$^{\circ}\text{C}$	40.1	19.1	8.5	6.3
Phase difference	$\Delta\phi$	rad	113.8	27.4	6.0	0.47
Distortion of a plane wave	$\frac{\Delta\phi}{2\pi}$	number of wavelengths	18.1	4.35	0.96	0.07
Critical temperature acc. to (8)	$\Delta T_c$	$^{\circ}\text{C}$	297	585	165	8.3
FOM <sub>TF</sub>	—	$10^3$ W	16.7	70.2	58.6	1.79
FOM <sub>D</sub>	—	$10^3$ W	0.18	0.26	1.2	15.2

#### 4 ANTIREFLECTION COATINGS

Using reflection characteristics and electric field strengths to act as evaluation standards, the three layer antireflection coating was designed.

$$\text{KCl} \left| 0.759 \frac{\lambda}{4} \text{ZnSe} - 0.538 \frac{\lambda}{4} \text{PbF}_2 - 0.388 \frac{\lambda}{4} \text{ZnSe} \right| \text{Air}$$

In this,  $\lambda = 10.6 \mu\text{m}$ . ZnSe and  $\text{PbF}_2$  optical constants at  $10.6 \mu\text{m}$  are, respectively,  $2.35 - 0.0001 i$  and  $1.55 - 0.0003 i$ . The design reflection rate is  $R=0.00\%$ . The absorption rate is  $A_c=0.03\%$ .

Technical requirements for the preparation of reflection reducing films include: (1) Opting for the use of newly polished KCl to act as substrate; (2) Use a thermal radiation source to evaporate ZnSe and  $\text{PbF}_2$ . The crucible is quartz. The heating is tungsten filament; (3) Introduce Ar ion assistance technology.

In order to study absorption associated with antireflection coatings, samples were taken and made into a stepped form. Each film layer had two steps. The first step thickness was very thin in order to facilitate analysis of surface absorption influences. The second step of each film layer was evaporated in an unbroken manner. Following this, a  $1.06 \mu\text{m}$  photothermal deflection measurement system was used to measure the absorption on each step. In conjunction with this, option was made for the use of KCl substrate calibrations associated with already known absorption rates. Measurement results are set out in Table 4. From Table 4, it is possible to know that, 1) Although there are some differences between surface absorptions of measurement samples and samples actually used, thin film boundary absorption, however, is greater than body absorption; 2) Low energy ion assistance (40eV) sample absorptions will be much smaller than standard techniques. The key reason is that adsorption

associated with moisture in the air is reduced. Water absorption drops. However, relatively high energy ion assistance bombardment (270eV) absorption clearly increases. The reason is changes in film layer chemical measurements; 3) Film layer absorption relative to KCl substrate will be much greater. Moreover, following increases in layer number, absorption increases.

/939

TABLE 4. COMPARISONS OF ABSORPTION BETWEEN INTERFACE AND VOLUME OF LAYERS WITH DIFFERENT PROCESSES

Process	Coating	Absorption, %
	Bare KCl Substrate	0.003
Conventional resistive evaporation	KCl 20 nm ZnSe Air	0.011
	KCl  $0.759 \frac{\lambda}{4}$ ZnSe Air	0.014
	KCl  $0.759 \frac{\lambda}{4}$ ZnSe-30 nm PbF <sub>2</sub>  Air	0.022
	KCl  $0.759 \frac{\lambda}{4}$ ZnSe- $0.538 \frac{\lambda}{4}$ PbF <sub>2</sub>  Air	0.025
	KCl  $0.759 \frac{\lambda}{4}$ ZnSe- $0.538 \frac{\lambda}{4}$ PbF <sub>2</sub> -20 nm ZnSe Air	0.025
	KCl  $0.759 \frac{\lambda}{4}$ ZnSe- $0.538 \frac{\lambda}{4}$ PbF <sub>2</sub> - $0.388 \frac{\lambda}{4}$ ZnSe Air	0.044
Ion-assisted resistive evaporation with Ar <sup>+</sup> -ion energy of 40 eV	KCl 20 nm ZnSe Air	0.007
	KCl  $0.759 \frac{\lambda}{4}$ ZnSe Air	0.008
	KCl  $0.759 \frac{\lambda}{4}$ ZnSe-30 nm PbF <sub>2</sub>  Air	0.011
	KCl  $0.759 \frac{\lambda}{4}$ ZnSe- $0.538 \frac{\lambda}{4}$ PbF <sub>2</sub>  Air	0.014
	KCl  $0.759 \frac{\lambda}{4}$ ZnSe- $0.538 \frac{\lambda}{4}$ PbF <sub>2</sub> -20 nm ZnSe Air	0.022
	KCl  $0.759 \frac{\lambda}{4}$ ZnSe- $0.538 \frac{\lambda}{4}$ PbF <sub>2</sub> - $0.388 \frac{\lambda}{4}$ ZnSe Air	0.027
Ion-assisted resistive evaporation with Ar <sup>+</sup> -ion energy of 270 eV	KCl 20 nm ZnSe Air	0.013
	KCl  $0.759 \frac{\lambda}{4}$ ZnSe Air	0.041
	KCl  $0.759 \frac{\lambda}{4}$ ZnSe-30 nm PbF <sub>2</sub>  Air	0.042
	KCl  $0.759 \frac{\lambda}{4}$ ZnSe- $0.538 \frac{\lambda}{4}$ PbF <sub>2</sub>  Air	0.044
	KCl  $0.759 \frac{\lambda}{4}$ ZnSe- $0.538 \frac{\lambda}{4}$ PbF <sub>2</sub> -20 nm ZnSe Air	0.047
	KCl  $0.759 \frac{\lambda}{4}$ ZnSe- $0.538 \frac{\lambda}{4}$ PbF <sub>2</sub> - $0.388 \frac{\lambda}{4}$ ZnSe Air	0.051



As far as sample transmission rates are concerned, Nicolet DX Fourier spectrometers are used to measure them. Transmission rates for coating samples plated on both sides can reach 99%.

CW CO<sub>2</sub> lasers with 4W power and Gauss radii ( $1/e^2$ ) of approximately 0.1mm are used to make rupture tests. Coating layers had no damage. The explanation for this was that damage threshold values were at least better than  $10^4 \text{W/cm}^2$ . Of course, window destruction is not only related to power densities. It is also related to total power. Due to the fact that 20kW lasers are subject to limitations, these experiments have not yet been carried out.

**Conclusion** Using KCl crystals to act as substrate, ZnSe-PbF<sub>2</sub>-ZnSe three layer antireflection coating plated on both sides seems to be feasible for use in 20kW CO<sub>2</sub> laser windows.

/940

#### REFERENCES

- [1] M. Sparus, Optical Distortion by Heated Window in High-Power Laser Systems. *J. Appl. Phys.*, 1971, **42** (12): 5029~5046
- [2] M. Mousler, High-Power Optics. *Opt. Eng.*, 1976, **15** (2): 158~165
- [3] M. Sparus, M. Cottis, Pressure-Induce Optical Distortion in Laser Windows. *J. Appl. Phys.*, 1973, **44** (2): 789~794
- [4] G. H. Shorman, G. Fraizier, Transmissive Optics for High Power CO<sub>2</sub> Laser: Practical Consideration. *Opt. Eng.* 1978, **17** (3): 235~231
- [5] A. Gasser, E. W. Kreutz, K. Wissenbach, Physical Aspects of Surface Processing with Laser Radiation. *Proc. SPIE*, 1988, **1**: 1020, 70~95
- [6] T. Miyata, B & D of optics for high power CO<sub>2</sub> lasers, in *Japanese National Program, SPIE*, 1986, **620**: 131~140
- [7] T. F. Deutsch, Laser Window Materials an Overview. *J. Electr. Material*, 1975, **4** (4): 663~717
- [8] S. J. Sheiden, L. V. Knight, J. M. Thorne, Laser-Induced Thermal Lens Effect: A New Theoretical Model. *Appl. Opt.*, 1982, **21** (9): 1663~1669
- [9] J. R. Whinnery, Laser Measuerment of Optical Absorption in Liquids. *Acc. Chem. Res.*, 1974, **7**: 225~230
- [10] H. E. Reedy, G. L. Herrit, Comparison of GaAs and ZnSe for High Power CO<sub>2</sub> Laser Optics. *Proc. SPIE*, 1988, **1020**: 180~191
- [11] J. A. Snage, *Infrared Optical Materials & Their Anti-reflection Coatings*. 1th ed. Adam. H. Hilger Ltd., Bristol, 1985: 50~73
- [12] A. Feldman, D. Horowitz, T. Mijata *et al.*, Photoelastic Constants of Potassion Chloride at 10.6  $\mu\text{m}$ . *Appl. Opt.*, 1977, **16**(11): 2925~2930

DISTRIBUTION LIST

DISTRIBUTION DIRECT TO RECIPIENT

<u>ORGANIZATION</u>	<u>MICROFICHE</u>
B085 DIA/RTS-2FI	1
C509 BALLOC509 BALLISTIC RES LAB	1
C510 R&T LABS/AVEADCOM	1
C513 ARRADCOM	1
C535 AVRADCOM/TSARCOM	1
C539 TRASANA	1
Q592 FSTC	4
Q619 MSIC REDSTONE	1
Q008 NTIC	1
Q043 AFMIC-IS	1
E051 HQ USAF/INET	1
E404 AEDC/DOF	1
E408 AFWL	1
E410 AFDTC/IN	1
E429 SD/IND	1
P005 DOE/ISA/DDI	1
P050 CIA/OCR/ADD/SD	2
1051 AFIT/LDE	1
P090 NSA/CDB	1
2206 FSL	1

Microfiche Nbr: FTD95C000174  
NAIC-ID(RS)T-0760-94